

New Photosafety Assessment Strategy Based on the Photochemical and Pharmacokinetic Properties of Both Parent Chemicals and Metabolites

Masashi Kato, Gen Suzuki, Hiroto Ohtake, Yoshiki Seto, and Satomi Onoue

Department of Pharmacokinetics and Pharmacodynamics, School of Pharmaceutical Sciences, University of Shizuoka, Suruga-ku, Shizuoka, Japan

Received April 29, 2015; accepted August 19, 2015

ABSTRACT

Photoreactivity and dermal/ocular deposition of compounds have been recognized as key considerations for evaluating the phototoxic risk of compounds. Because some drugs are known to cause phototoxic reactions via generation of potent phototoxic metabolites, photosafety assessments on parent drugs alone may lead to false predictions about their photosafety. This study aimed to establish a new photosafety assessment strategy for evaluating the *in vivo* phototoxic potential of both a parent substance and its metabolites. The *in vivo* phototoxic risk of fenofibrate (FF) and its metabolites, fenofibric acid (FA) and reduced fenofibric acid, were evaluated based on photochemical and pharmacokinetic analyses. FF and FA exhibited intensive UV absorption, with molar extinction coefficient values of 17,000 (290 nm) and 14,000 M⁻¹cm⁻¹ (295 nm), respectively. Superoxide

generation from FA was significantly higher than from FF, and a marked increase in superoxide generation from FF was observed after incubation with rat hepatic S9 fractions, suggesting enhanced photoreactivity of FF after metabolism. FA showed high dermal/ocular deposition after oral administration (5 mg/kg, *p.o.*) although the concentration of FF was negligible, suggesting high exposure risk from FA. On the basis of these findings, FA was deduced to be a major contributor to phototoxicity induced by FF taken orally, and this prediction was in accordance with the results from *in vitro/in vivo* phototoxicity tests. Results from this study suggest that this new screening strategy for parent substances and their metabolites provides reliable photosafety information on drug candidates and would be useful for drug development with wide safety margins.

Introduction

Drug-induced photosensitivity can be elicited by topical or systemic application of pharmaceutical substances in combination with subsequent exposure to sunlight or artificial light (Moore, 2002; Drucker and Rosen, 2011). Because the photochemical reactions of drug molecules are a key trigger of phototoxic reactions, photochemical evaluations such as UV spectral analysis and reactive oxygen species (ROS) assays are carried out as photosafety assessments in pharmaceutical research to avoid adverse phototoxic events (Onoue et al., 2009; Seto et al., 2012). In addition to photochemical evaluation, pharmacokinetic (PK) evaluation with a focus on sunlight-exposed tissues (e.g., skin and eyes) can also be helpful for predicting *in vivo* phototoxicity, because phototoxic reactions mainly occur in the skin (Seto et al., 2009, 2011). Currently, regulatory agencies recommend PK characterization as well as photochemical characterization for photosafety assessment of pharmaceuticals. For example, tissue distribution

is recommended in the guidelines for photosafety assessment of pharmaceuticals published by the International Conference on Harmonisation of Technical Requirements for Registration of Pharmaceuticals for Human Use (ICH) in 2014.

In many cases of drug-induced photosensitivity, phototoxic reactions are thought of as mainly being elicited by parent drugs, and the photosafety of drug metabolites is, in principle, outside the scope of regulatory oversight (according to the 2014 ICH S10 guideline). However, the metabolites of phototoxic compounds can have phototoxicity that is as potent as that of their parent drugs, and some metabolites have even more potent phototoxic potential than their parent chemicals, including amiodarone, chlorpromazine, and fenofibrate (FF) (Ljunggren, 1977; Ljunggren and Möller, 1977; Ferguson et al., 1985; Miranda et al., 1994). In our previous investigation, *in vivo* phototoxic risk of chlorpromazine was predicted to be less phototoxic on the basis of the photochemical and PK characteristics of its parent compounds, although a potent *in vivo* phototoxic reaction was in fact observed in the rat skin after oral administration of chlorpromazine (Onoue et al., 2014a). Previous studies have shown that chlorpromazine taken orally is extensively metabolized by cytochrome P450 (Wójcikowski et al., 2010), and its demethylated metabolites are more phototoxic than chlorpromazine (Ljunggren and Möller, 1977). In this context, false predictions might

This research was supported in part by the Ministry of Health, Labour and Welfare of Japan [Health Labour Sciences Research Grant H25-iyaku-wakate-024], the Cosmetology Research Foundation [Grant 527], and the Hoya Science Foundation [Grant 31].

dx.doi.org/10.1124/dmd.115.065060.

ABBREVIATIONS: 3T3 NRU PT, 3T3 neutral red uptake phototoxicity test; AUC_{0-∞}, area under the concentration versus time curve from time 0 to ∞ after administration; DMSO, dimethylsulfoxide; FA, fenofibric acid; FF, fenofibrate; ICH, International Conference on Harmonisation of Technical Requirements for Registration of Pharmaceuticals for Human Use; MEC, molar extinction coefficient; MPE, mean photo effect; mROS, micellar reactive oxygen species; NBT, nitroblue tetrazoleum; PK, pharmacokinetic; QN, quinine; RFA, reduced fenofibric acid; ROS, reactive oxygen species; SB, sulisobenzone; UPLC/ESI-MS, ultra-performance liquid chromatography equipped with electrospray ionization mass spectrometry.

arise from the lack of photochemical and PK characterization of metabolites, and the photosafety assessments of metabolites as well as their parent chemicals should provide more reliable photosafety information on pharmaceuticals; however, the feasibility of such new screening strategies is unknown.

This study aimed to establish a new photosafety assessment strategy with the combined use of photochemical and PK characterization on a parent drug and its metabolites, applying this new screening strategy to FF and its major metabolites, fenofibric acid (FA) and reduced fenofibric acid (RFA) (Fig. 1). FF, an antihyperlipoproteinemic agent, is clinically recognized as phototoxic (Roberts, 1989; Leenutaphong and Manuskiatti, 1996; Machet et al., 1997), and the phototoxic potential of FF has been investigated using several *in vitro* tools, demonstrating the potent *in vitro* phototoxicity of FF and FA (Vargas et al., 1993; Miranda et al., 1994). Thus, in this study, FF and its metabolites were employed as model chemicals to confirm the feasibility of the new screening strategy. The photoreactivity of these compounds was evaluated by UV spectral analyses and ROS determination before and after incubation with rat hepatic/intestinal S9 fractions. Dermal and ocular deposition of FF and its metabolites was characterized after the oral administration of FF to rats.

Materials and Methods

Chemicals. FF was purchased from Wako Pure Chemical Industries (Osaka, Japan). FA and RFA were bought from AK Scientific Inc. (Union City, CA) and Toronto Research Chemicals Inc. (Toronto, Ontario, Canada), respectively. Pooled IGS Sprague-Dawley rat liver S9 fractions, pooled IGS Sprague-Dawley rat intestinal S9 fractions, and an NADPH-regenerating system were obtained from Sekisui Medical (Tokyo, Japan). All other reagents were purchased from commercial sources. A quartz reaction container for irradiation of simulated sunlight to a 96-well plate was constructed by Ozawa Science (Aichi, Japan).

UV Spectral Analysis. UV spectral analysis was performed as previously described (Seto et al., 2013b) with minor modifications. Briefly, FF (20 μ M) was

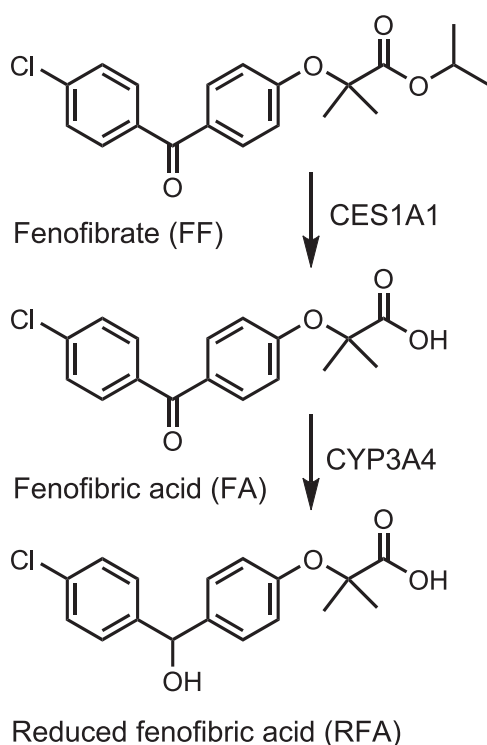


Fig. 1. Major metabolic pathways of FF in rats, monkeys, and humans. FF is metabolically transformed into FA and RFA (Miller and Spence, 1998; Fukami et al., 2010).

not dissolved in 20 mM sodium phosphate buffer (NaPB, pH 7.4) due to its poor solubility; thus, each compound was dissolved in ethanol at a final concentration of 20 μ M. UV absorption spectra were recorded with a Hitachi U-2010 spectrophotometer (Hitachi High-Technologies Corporation, Tokyo, Japan) interfaced to a PC for data processing (Spectra Manager software; JASCO, Easton, MD). A spectrofluorometer quartz cell with a 10-mm pathlength was employed. Molar extinction coefficient (MEC) values were calculated on the basis of maximum absorbance values in the wavelength range of 290–400 nm.

Irradiation Conditions for Determination of ROS. An Atlas Suntest CPS+ (Atlas Material Technology LLC, Chicago, IL) equipped with a 1500 W xenon arc lamp and a SR-P20FLE cooling unit (Hitachi, Tokyo, Japan) was used to determine ROS from irradiated chemicals. A UV special filter was installed to adapt the spectrum of the artificial light source to that of natural daylight; the Atlas Suntest CPS series has a high irradiance capability that meets International Commission on Illumination CIE85/1989 daylight simulation requirements. The irradiation test was carried out at 25°C with an irradiance of approximately 2.0 mW/cm² as determined with a calibrated Dr. Hönle 0037 UVA detector (Munich, Germany).

Determination of ROS from Photoirradiated Compounds. Determination of singlet oxygen and superoxide generated from photoirradiated compounds was conducted in accordance with an established protocol (Seto et al., 2013a). Briefly, each tested compound was dissolved in dimethylsulfoxide (DMSO) at 10 mM as a stock solution. To monitor the generation of singlet oxygen, samples containing compounds (200 μ M), *p*-nitrosodimethylaniline (50 μ M), and imidazole (50 μ M) in 20 mM NaPB (pH 7.4) with 0.5% (v/v) Tween 20 were irradiated with simulated sunlight, and then the UV absorption at 440 nm was measured using the Safire plate reader (TECAN, Männedorf, Switzerland). To determine superoxide generation, samples containing the compounds (200 μ M) and nitroblue tetrazolium (NBT; 50 μ M) in 20 mM NaPB (pH 7.4) with 0.5% (v/v) Tween 20 were exposed to simulated sunlight, and the reduction of NBT was measured by the increase in the absorbance at 560 nm using the Safire plate reader. According to the results (mean of triplicate determinations) from the micellar reactive oxygen species (mROS) assay, photoreactivity for each tested chemical should be judged to be 1) positive with singlet oxygen ($\Delta A_{440\text{ nm}} \times 10^3$): 25 or more, and/or superoxide ($\Delta A_{560\text{ nm}} \times 10^3$): 20 or more; or 2) negative with singlet oxygen ($\Delta A_{440\text{ nm}} \times 10^3$): less than 25, and superoxide ($\Delta A_{560\text{ nm}} \times 10^3$): less than 20. In the mROS assay, the final decision should be made as follows: 1) positive: above the threshold level for singlet oxygen or superoxide; or 2) negative: below the threshold level for both singlet oxygen and superoxide (Onoue et al., 2013a).

Determination of ROS from Photoirradiated Compounds in Enzyme-Treated Samples. Rat hepatic/intestinal S9 fractions were preincubated for 2 minutes at 37°C (final concentration: 0.2 mg protein/ml) in 0.3 ml phosphate buffer (pH 7.4) containing typical cofactors. FF was dissolved in DMSO at 10 mM as a stock solution. The reaction was initiated by the addition of FF at 100 μ M, and the final concentration of DMSO was 1%. The reaction was terminated at 1 minute by adding 0.2 ml ice-cold ethanol. For comparison, FF (100 μ M) was also incubated with heat-inactivated (approximately 80°C, 5 minutes) S9 fractions (denatured groups). The mixtures were evaluated by a ROS assay (Onoue et al., 2013a). Briefly, to monitor the generation of singlet oxygen, enzyme-treated mixtures, *p*-nitrosodimethylaniline (50 μ M), and imidazole (50 μ M) was dissolved in 20 mM NaPB (pH 7.4). To determine superoxide generation, the enzyme-treated mixtures and NBT (50 μ M) were dissolved in 20 mM NaPB (pH 7.4). Both reaction mixtures theoretically contained 50 μ M FF. These samples were then irradiated with simulated sunlight and measured in the same conditions as with the ROS assay protocol.

Animals. Male Sprague-Dawley rats aged 11 to 12 weeks (approximately 300–350 g body weight) were purchased from SLC Inc. (Hamamatsu, Japan). For PK experiments, rats ($n = 39$) were fasted for approximately 18 hours before drug administration and orally received an ethanolic solution of FF at a dose of 5 mg/kg. For *in vivo* phototoxicity testing, rats ($n = 16$) were anesthetized using pentobarbital (50 mg/kg *i.p.*), and then the hair on the abdomen was shaved at approximately 18 hours before dermal application of the drug solution. All of the procedures used in this study were conducted according to the guidelines approved by the Institutional Animal Care and Ethical Committee of University of Shizuoka.

PK Studies. Blood samples were taken in a volume of 200 μ l from the tail vein at the indicated periods (0.5, 1, 2, 3, 4, 6, 8, 12, 24, and 48 hours) after drug administration. The blood samples were centrifuged (10,000 \times g, 10 minutes, 4°C) to prepare plasma

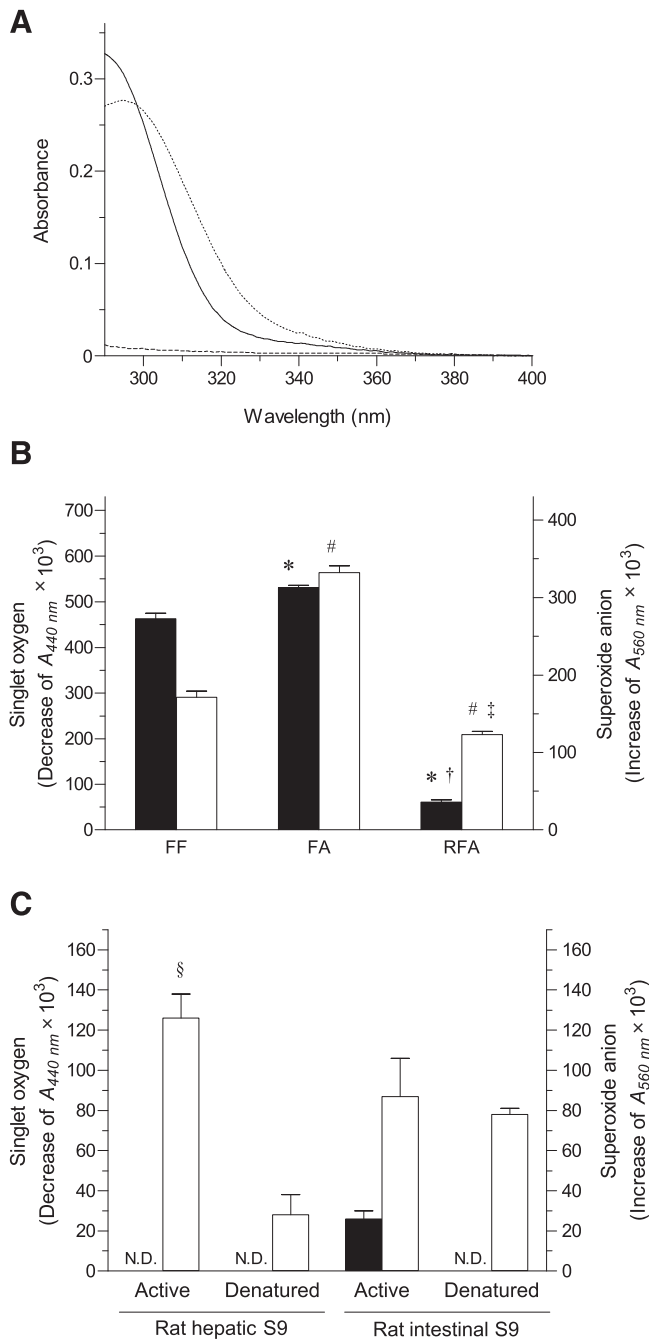


Fig. 2. Photochemical properties of FF and metabolites. (A) UV absorption spectra of compounds (20 μM) in ethanol. Solid line, FF; dashed line, RFA; dotted line, FA. (B) Generation of ROS from each test compound (200 μM). Filled bars, generation of singlet oxygen; open bars, generation of superoxide. * $P < 0.05$ versus FF within singlet oxygen; † $P < 0.05$ versus FA within singlet oxygen; # $P < 0.05$ versus FF within superoxide; ‡ $P < 0.05$ versus FA within superoxide. Data represent the mean \pm S.D. ($n = 3$). (C) Generation of ROS from enzyme-treated FF. § $P < 0.05$ versus superoxide in denatured rat hepatic S9 fractions. Data represent the mean \pm S.D. ($n = 3$). N.D., not detected.

samples, and then the samples (100 μl) were deproteinized by the addition of acetonitrile (250 μl). The supernatants were obtained by centrifugation (2000 rpm, 1 minute, 4°C) and filtration (0.20- μm membrane filter, Millex-LG; Millipore, Billerica, MA) and were kept frozen at -20°C until they were analyzed.

At the indicated times (2, 4, 6, 8, 10, 12, 24, and 48 hours) after oral administration of FF, rats were humanely euthanized by taking blood from the descending aorta under anesthesia with pentobarbital Na (50 mg/kg), and the tissues were then perfused with cold saline from the aorta. The skin and eye were

dissected, minced with scissors, and homogenized using Physcotron (Microtec, Chiba, Japan) in 4 ml acetonitrile. After sonication for 10 minutes and shaking for 10 minutes, the samples were centrifuged (3000 rpm, 10 minutes). Extraction was repeated twice with acetonitrile, and the supernatants were pooled. The collected eluents were pooled with acetonitrile extracts, and the samples were evaporated to dryness under a gentle stream of nitrogen at 45°C. The extracted and evaporated tissue samples were stored at 4°C until they were analyzed.

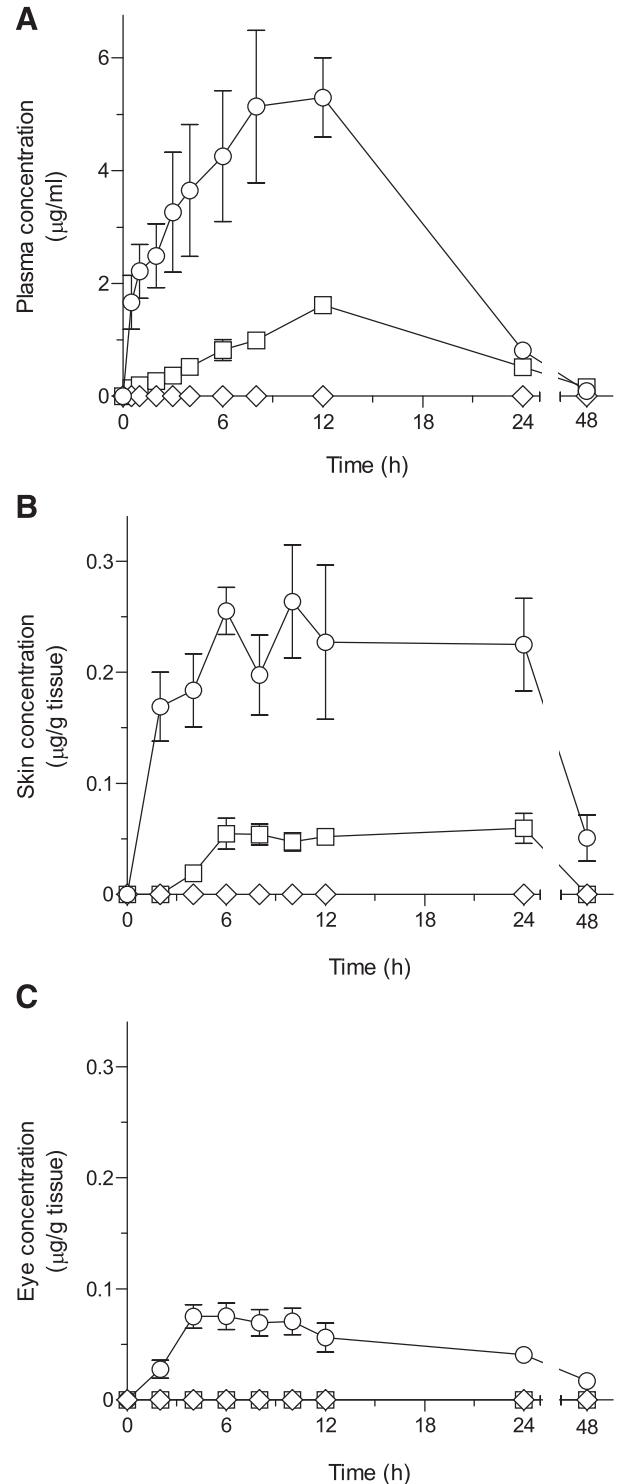


Fig. 3. Concentration-time profiles of FF, FA, and RFA after oral administration of FF (5 mg/kg) in rats. (A–C) Concentrations in plasma (A), skin (B), and eyes (C). Open diamonds, FF; open circles, FA; open squares, RFA. Data represent the mean \pm S.E.M. ($n = 4$ –7).

TABLE 1
Pharmacokinetic parameters in plasma, skin, and eyes after oral administration of fenofibrate in rats

Samples	$t_{1/2}$ (h)	C_{max} ($\mu\text{g/ml}$ or $\mu\text{g/g}$ tissue)	T_{max} (h)	$AUC_{0-\infty}$ ($\text{h} \cdot \mu\text{g/ml}$ or $\text{h} \cdot \mu\text{g/g}$ tissue)	MRT (h)
FF					
Plasma	N.A.	N.A.	N.A.	N.A.	N.A.
Skin	N.A.	N.A.	N.A.	N.A.	N.A.
Eye	N.A.	N.A.	N.A.	N.A.	N.A.
FA					
Plasma	6.4 ± 0.40	6.3 ± 1.1	9.7 ± 1.1	97 ± 14	13 ± 0.70
Skin	11 ± 1.5	0.34 ± 0.017	13 ± 3.9	8.5 ± 1.3	20 ± 2.1
Eye	22 ± 6.9	0.10 ± 0.0055	6.0 ± 1.4	2.6 ± 0.33	34 ± 10
RFA					
Plasma	12 ± 1.0	1.6 ± 0.10	12 ± 0.0	33 ± 3.2	21 ± 1.5
Skin	17 ± 3.3	0.080 ± 0.0067	16 ± 4.7	2.0 ± 0.60	30 ± 4.2
Eye	N.A.	N.A.	N.A.	N.A.	N.A.

$AUC_{0-\infty}$, area under the concentration vs. time curve from $t=0$ to $t=\infty$ after administration; C_{max} , maximum concentration; $t_{1/2}$, terminal half-life; T_{max} , time to maximum concentration; and MRT, mean residence time. Each value represents the mean \pm SEM for 4–7 rats. N.A., not available due to concentrations below the limit of detection.

To determine drug concentrations in plasma and tissue samples, an ultra-performance liquid chromatography equipped with electrospray ionization mass spectrometry (UPLC/ESI-MS) system was employed (Onoue et al., 2013b). The UPLC-ESI/MS system consisted of a Waters Acquity UPLC system (Waters, Milford, MA), which included a binary solvent manager, a sample manager, a column compartment, and a micromass SQ detector connected with Waters MassLynx (version 4.1). A Waters Acquity UPLC BEH C18 column (particle size, $1.7 \mu\text{m}$; and column size, $\Phi 2.1 \times 50 \text{ mm}$; Waters) was used, and the column temperature was maintained at 40°C . The deproteinized plasma samples were mixed with 50% acetonitrile solution containing ketoprofen ($1 \mu\text{g/ml}$), an internal standard for UPLC/ESI-MS analysis (1:1 ratio of supernatant/ketoprofen). To determine tissue concentration, the extracted and evaporated samples were dissolved in 50% acetonitrile including ketoprofen (500 ng/ml). The standards and samples were separated using a gradient mobile phase consisting of purified water containing 0.1% formic acid (A) and acetonitrile (B). The gradient conditions of the mobile phase were as follows: 0 to 1.0 minute, 50% B; 1.0 to 5.0 minutes, 50% to 95% B (linear gradient curve); 5 to 5.5 minutes, 95% B; and 5.5 to 6 minutes, 50% B. The flow rate was set at 0.25 ml/min . Analyses were carried out by monitoring specific mass-to-charge ratios as follows: $361.2 [\text{M} + \text{H}]^+$ for FF, $319.2 [\text{M} + \text{H}]^+$ for FA, $303 [\text{M} - \text{OH}]^+$ for RFA, and $255.2 [\text{M} + \text{H}]^+$ for ketoprofen (internal standard).

3T3 Neutral Red Uptake Phototoxicity Testing. Balb/c 3T3 mouse fibroblast cells (CloneA-31) were maintained in culture as previously reported (Spielmann et al., 1991). The 3T3 neutral red uptake phototoxicity test (3T3 NRU PT) and data analyses were carried out as described in the 2004 Organisation for Economic Co-operation and Development Guideline 432. Briefly, Balb/c 3T3 cells were maintained in culture for 24 hours for the formation of monolayers. Two 96-well plates per test chemical were then preincubated with six different concentrations of the chemical dissolved in Earle's balanced salt solution for 1 hour in duplicate. One plate was then exposed to a dose of 5 J/cm^2 UVA (irradiation experiment), whereas the other plate was kept in the dark by covering it with aluminum foil (nonirradiation experiment). UVA irradiation (approximately 30 minutes) was performed using a SOL 500 Sun simulator (Dr. Hönle) equipped with a 500 W metal halide lamp and an H-1 filter to remove potentially cytotoxic UVB wavelengths. The treatment medium was then replaced with culture medium; after 24 hours, cell viability was determined by neutral red uptake for 3 hours. After that, cells were lysed in eluate (50:49:1 ratio of ethanol/water/acetic acid), and neutral red uptake was measured at an absorbance of 540 nm using the Benchmark Plus microplate spectrophotometer (BioRad, Hercules, CA). Cell viability obtained with each of the six concentrations of the test chemical was compared with that of untreated controls, and mean photo effect (MPE) values were calculated by using Phototox software (version 2.0; ZEBET, Berlin, Germany) on the basis of obtained cell viability curves in UVA-irradiated and nonirradiated groups of the test chemical for evaluating in vitro phototoxicity.

In Vivo Phototoxicity Testing. Experiments were performed as described previously, with minor changes in dermal administration (Seto et al., 2009). Each FF, FA, or control [quinine (QN) and sulisobenzone (SB)] was dissolved in

DMSO at 100 mg/ml and was applied to two application sites on rat skin at the abdomen (10 mg/site , $n = 4$) using filter paper ($2 \text{ cm} \times 2 \text{ cm}$) under anesthesia with pentobarbital Na (50 mg/kg). At 4 hours after dermal administration, the filter papers containing chemicals on the application sites were removed and wiped using cotton soaked with distilled water. Rats were then irradiated individually using black light (FL15BL-B; National, Tokyo, Japan) as a UVA light source with an irradiance of approximately 2.7 mW/cm^2 for approximately 3 hours until the UV irradiance level reached 30 J/cm^2 . Because UVB light is highly cytotoxic, a UVA light source was employed for the in vivo phototoxicity testing. During the UVA irradiation, rats were restrained on a sunbed under anesthesia with pentobarbital Na (50 mg/kg) to ensure uniform irradiation of their abdomen, and nonirradiated sites were wrapped in aluminum foil for protection from UV light. UV intensity was monitored using the calibrated Dr. Hönle 0037 UVA detector. A colorimeter equipped with a data processor (NF333; Nippon Denshoku, Tokyo, Japan) was used as a measure of skin color. This instrument records three-dimensional color reflectance, the so-called $L^*a^*b^*$ system, as recommended by the International Commission on Illumination. The luminance (L^*) gives the relative brightness ranging from total black ($L^* = 0$) to total white ($L^* = 100$). The hue (a^*) axis represents the balance between red (positive values up to 100) and green (negative values up to -100), and the chroma (b^*) axis represents the balance between yellow (positive values up to 100) and blue (negative values up to -100). The differences in skin color (ΔE) between before and after irradiation were described as follows (Westerhof et al., 1986; Piérard and Piérard-Franchimont, 1993):

$$\Delta E = \sqrt{(\Delta L^*)^2 + (\Delta a^*)^2 + (\Delta b^*)^2}$$

Data Analysis. The significance of differences was determined by t tests on the data from ROS generation after incubation with rat hepatic/intestinal S9 fractions. Other data were analyzed by one-way analysis of variance followed by Tukey's multiple comparison tests. $P < 0.05$ was considered significant for all analyses. PK characterizations were performed by noncompartmental analysis as implemented in WinNonlin Professional software (version 5.2; Pharsight Corporation, Mountain View, CA).

Results

Photochemical Characterization. Phototoxic reactions can be triggered by photochemical reactions of drug molecules after absorption of UV and visible light (290–700 nm) (Moore, 1998; Onoue and Tsuda, 2006). Herein, the photochemical properties of FF and two major metabolites, FA and RFA, were analyzed with a focus on UV-absorbing properties and ROS-generating potentials. FF and FA exhibited intensive UVA/UVB absorption, with maximal MEC values of $17,000$ (290 nm) and $14,000 \text{ M}^{-1} \text{ cm}^{-1}$ (295 nm); by contrast, only weak

UVB absorption was observed in RFA, with an MEC of $850 \text{ M}^{-1}\text{cm}^{-1}$ at 290 nm (Fig. 2A). Drug molecules with an MEC of less than $1000 \text{ M}^{-1}\text{cm}^{-1}$ were previously demonstrated to be less phototoxic (Henry et al., 2009); thus, FF and FA can be identified as photoexcitable.

To clarify the photoreactivity of FF and its metabolites, the generation of ROS from these compounds ($200 \mu\text{M}$) was determined under irradiation of simulated sunlight (Fig. 2B) since the good relationship between ROS data on chemicals at $200 \mu\text{M}$ and in vivo phototoxicity revealed the prediction capacity of the ROS assay (Onoue and Tsuda, 2006; Onoue et al., 2008a). FF and FA exhibited potent generation of singlet oxygen, with values of 463 and 531 ($\Delta A_{440 \text{ nm}} \times 10^3$), respectively; they also generated superoxide, with values of 171 and 332 ($\Delta A_{560 \text{ nm}} \times 10^3$). The levels of ROS generation from RFA were lower than those from FF and FA, and the values of singlet oxygen and superoxide generation were 61 ($\Delta A_{440 \text{ nm}} \times 10^3$) and 123 ($\Delta A_{560 \text{ nm}} \times 10^3$), respectively. From these findings, all compounds were judged to be photoreactive according to the ROS data-based classification system, and the photoreactivity of the compounds was ranked as follows: $\text{FA} > \text{FF} \gg \text{RFA}$.

ROS generation from enzyme-treated FF was determined after incubation with rat hepatic/intestinal S9 fractions to evaluate the possible photochemical transitions of FF after metabolism (Fig. 2C). Although no significant differences were observed in ROS generation from FF between pretreatment of active and denatured rat intestinal S9 fractions, the generation of superoxide from FF was significantly increased by approximately 4.5-fold after preincubation with active rat hepatic S9 fractions compared with that from FF incubated with the denatured one ($P < 0.05$), suggesting enhanced photoreactivity of FF after metabolism in the liver.

PK Characterization. Phototoxic reactions mainly occur in the skin and eyes; thus, dermal and ocular exposure to compounds can be a predictive factor for in vivo phototoxicity as well as systemic exposure (Boiy et al., 2008; Seto et al., 2009). PK characterizations of compounds were conducted with a focus on plasma, skin, and eyes (Fig. 3; Table 1). After oral administration of FF to rats, FF was negligible in all tissues (below the limit of detection: 10 ng/ml and 7.1 ng/g tissue), whereas its metabolites could be detected in plasma and tissues. A rapid and sustained increase in the FA level was observed in all tissues up to 6.0–13 hours, whereas RFA concentrations in the plasma and skin were gradually elevated (T_{max} of 12–16 hours). The C_{max} and area under the concentration versus time curve from time 0 to ∞ after administration ($\text{AUC}_{0-\infty}$) values in plasma and skin of FA were approximately 3- to 4-fold higher than those of RFA, and only FA could be detected in rat eyes, with C_{max} and $\text{AUC}_{0-\infty}$ values of $0.10 \mu\text{g/g}$ tissue and $2.6 \text{ h} \cdot \mu\text{g/g}$ tissue, respectively. Therefore, FA would have a higher exposure risk of UV-exposed tissues compared with RFA. By contrast, RFA exhibited slower elimination from the plasma and skin compared with FA, as evidenced by the approximately 1.5- to 2-fold-longer apparent half-lives of RFA compared with FA in the plasma and skin, suggesting longer tissue retention of RFA. From the PK characteristics, dermal and ocular exposure was ranked as follows: $\text{FA} > \text{RFA} \gg \text{FF}$.

Comparative In Vitro/In Vivo Photosafety Assessments. When both photochemical and PK data are taken into account, FA was more likely to be phototoxic than the others; the photosafety of FA was then examined by both 3T3 NRU PT, a well validated alternative method for photosafety assessment (Spielmann et al., 1998), and the rat in vivo phototoxicity test. FF was also tested for comparison. QN and SB were employed as positive/negative controls in both in vitro/in vivo photosafety tests, respectively. In 3T3 NRU PT, cell viability curves were almost identical between UV-irradiated and nonirradiated groups treated with SB (Fig. 4A). By contrast, QN induced potent phototoxicity

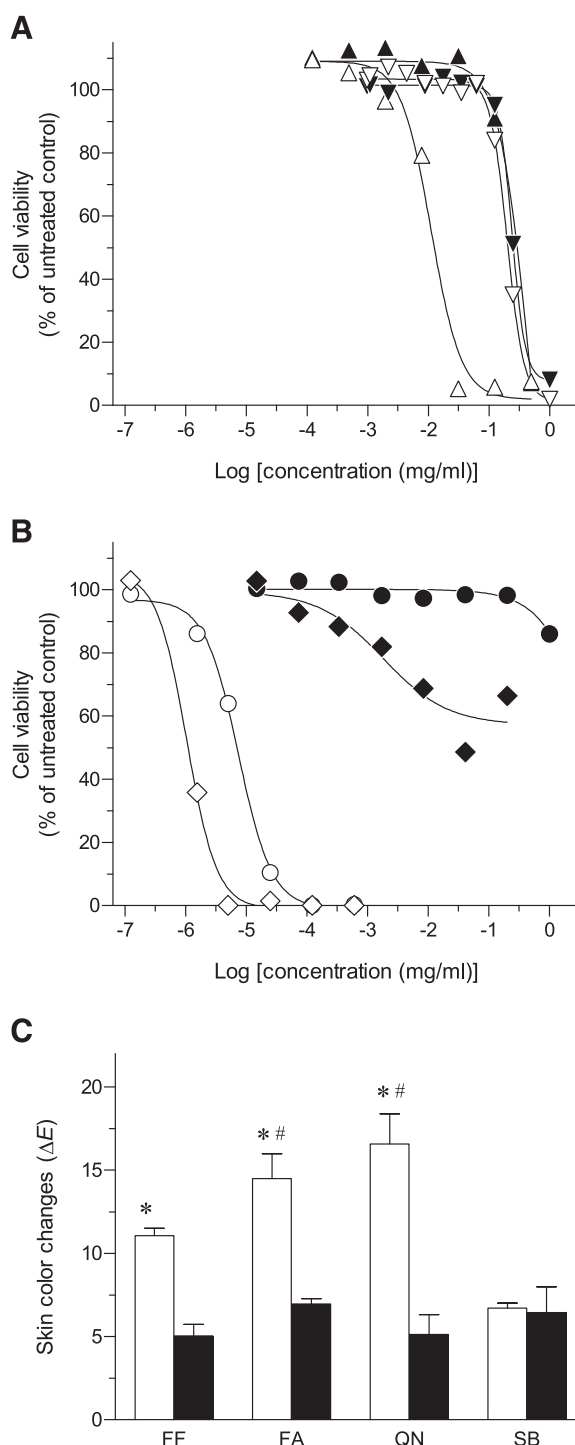


Fig. 4. In vitro/in vivo phototoxicity tests on QN, SB, FF, and FA. (A and B) 3T3 NRU phototoxicity testing on positive/negative controls (A) and FF and FA (B). Upward triangles, QN; downward triangles, SB; diamonds, FF; circles, FA. Open symbols, UV-irradiated groups; filled symbols, nonirradiated groups. Data represent the mean of duplicate measurements. (C) Colorimetric evaluation (ΔE) of phototoxic skin responses in rats. Open bars, UV-irradiated groups; filled bars, nonirradiated groups. * $P < 0.05$ versus the nonirradiated group of each compound; # $P < 0.05$ versus SB within UV-irradiated groups. Data represent the mean \pm S.E.M. ($n = 4$).

to 3T3 cells after UV irradiation. As observed for QN, FF and FA also exhibited enhanced cell death upon UV exposure, indicating potent phototoxicity to 3T3 cells (Fig. 4B). MPE values can distinguish phototoxic molecules ($\text{MPE} \geq 0.1$) from nonphototoxic ones ($\text{MPE} < 0.1$) (Holzhutter, 1997), and MPE values of FF and FA were 0.40 and

0.54, respectively. Therefore, both FF and FA were identified as phototoxic, and FA would be more phototoxic to 3T3 cells than FF because of its larger MPE value.

In vivo photosafety profiles were assessed based on the transitions in skin color (ΔE) after UV irradiation after dermal administration of FF, FA, QN, and SB (Fig. 4C). Dermal concentrations of FF and FA did not increase from 2 to 6 hours after dermal application (data not shown), suggesting steady-state concentrations of the drugs in the skin; then, the application period was confirmed at 4 hours in this study. In SB-treated groups, no significant differences were observed between UV-irradiated and nonirradiated rats. On the other hand, upon UV irradiation, QN induced a significant increase in the ΔE value owing to the increase in the Δb^* value, as previously observed (Nose and Tsurumi, 1993). UV-irradiated FF and FA also exhibited significantly higher ΔE values than each nonirradiated group ($P < 0.05$), and these color changes were due to significant increases of Δb^* values by 6.4 (for FF) and 5.9 (for FA). Furthermore, in FA-treated groups, the Δa^* value was also significantly increased by 4.7 upon UV irradiation. Although ΔE values were not significantly different between UV-irradiated FF and UV-irradiated SB, the ΔE value of UV-exposed rats treated with FA was significantly higher than that of UV-exposed rats treated with SB ($P < 0.05$). These results demonstrated more severe phototoxicity of FA than FF to rat skin.

Discussion

To evaluate in vivo phototoxic risk of a chemical and its metabolites, development of a new photosafety screening system was attempted by photochemical and PK characterization, and the new screening strategy was applied to predict in vivo phototoxic risk of FF and its major metabolites, FA and RFA. According to our outcomes, FA, a major metabolite of FF, can be the major contributor to FF-induced phototoxic skin responses because of its potent photoreactivity and high dermal/ocular exposure.

The primary trigger for phototoxic reactions can be photoexcitation of chemical molecules with UV/visible light irradiation (Moore, 1998); and excited molecules then tend to undergo type I and/or II photochemical reactions with molecular oxygen and/or biomolecules. Generation of superoxide and singlet oxygen from photoirradiated chemicals can be reliable indicators of type I and II photochemical reactivity, respectively (Onoue and Tsuda, 2006; Onoue et al., 2008a).

From the ROS data, type I reactivity of FA was higher than that of FF; on the other hand, photoreactivity of RFA would be low among tested chemicals. In addition, enhanced superoxide generation could be observed after preincubation of FF with active rat hepatic S9 fractions compared with the denatured group. Benzophenones including FF and FA can elicit lipid peroxidation, a major mechanism of photoirritation, via type I photochemical reactions after photoexcitation (Marković et al., 1990). In this context, FA might be a major contributor to FF-induced phototoxicity after metabolism of FF. For photosafety assessments, exposure of compounds and their retention to dermal/ocular tissues can also be a key consideration because phototoxic reactions typically occur in the skin and eyes (Boiy et al., 2008; Seto et al., 2009). Therefore, in this study, the PK behavior of FF and its metabolites was assessed with a focus on plasma and skin/eyes in rats after oral administration of FF. Interestingly, FF was negligible in all samples, and only two metabolites could be detected in our PK study. According to our results, FA would have the highest dermal/ocular exposure risk, suggesting a major contribution of FF-induced phototoxicity. Although dermal exposure risk of RFA was lower than FA, RFA might have longer-term dermal exposure risk compared with FA on the basis of its long elimination half-life. For comparison, in vitro/in vivo phototoxicity tests were also conducted, and potent phototoxicity of FF and FA was confirmed. According to the cell viability curves and ΔE values in UV-irradiated groups, the metabolic activity for conversion of FF to FA might not be high in 3T3 cells and rat skin; phototoxicity of FA would be more potent than that of FF on the basis of the data obtained.

In photosafety assessment, both photochemical and PK properties should be taken into consideration; thus, a summary table was built using photochemical and PK data (Table 2), and values among the data are classified as high, moderate, and low levels in accordance with our previous research (Seto et al., 2011). In our photosafety prediction, high levels for both photochemical and PK data might indicate high phototoxic potential, whereas low levels in either or both might be indicative of moderate or low phototoxic potential. FA was deduced to be a highly phototoxic metabolite because both photoreactivity and dermal/ocular exposure were high. FF and RFA were less phototoxic, owing to limited dermal/ocular exposure of FF, moderate photoreactivity, and limited ocular exposure of RFA. In this context, the phototoxic risk of test compounds was deduced as follows: FA \gg RFA $>$ FF (in the skin) and FA \gg RFA = FF (in the eyes). The deduced phototoxic potential of FF and FA was in

TABLE 2
Decision matrix for evaluating in vivo phototoxicity risk of FF and its metabolites

Assays	FF		FA		RFA	
	Value	Level of Intensity	Value	Level of Intensity	Value	Level of Intensity
Photochemical properties						
UV absorbance						
λ_{\max} (nm) [ϵ ($M^{-1}cm^{-1}$)]	290 [17,000]	High	295 [14,000]	High	290 [850]	Low
ROS data						
1O_2 ($\Delta A_{440\text{ nm}} \times 10^3$)	463	High	531	High	61	Low
O_2^- ($\Delta A_{560\text{ nm}} \times 10^3$)	171	Moderate	332	High	123	Moderate
Distribution to UV-exposed tissues						
Skin						
$t_{1/2}$ (h)	N.A.		11	Moderate	17	High
C_{\max} ($\mu g/g$ tissue)	N.A.		0.34	High	0.080	Low
$AUC_{0-\infty}$ ($h \cdot \mu g/g$ tissue)	N.A.		8.5	High	2.0	Moderate
Eyes						
$t_{1/2}$ (h)	N.A.		22	High	N.A.	
C_{\max} ($\mu g/g$ tissue)	N.A.		0.10	Moderate	N.A.	
$AUC_{0-\infty}$ ($h \cdot \mu g/g$ tissue)	N.A.		2.6	Moderate	N.A.	

Each crucial factor was divided into three levels of intensity, which are indicated as low, medium, and high. N.A., not available due to concentrations below the limit of detection.

agreement with the phototoxic outcomes from in vitro/in vivo photosafety tests, suggesting the reliability of our photosafety prediction on FF and FA. From these findings, phototoxic events related to FF would be attributed to FA, which might be the reason for the discrepancy between the observed phototoxicity after oral administration and the negative results in the photopatch test of FF (Leenutaphong and Manuskiatti, 1996).

Many drugs seemed to exhibit different PK behavior between humans and nonhuman primates, which may partly be due to species differences of metabolic enzymes such as cytochrome P450 enzymes, esterases, and glucuronidases (Baillie and Rettie, 2011). FF is metabolized into FA by carboxylesterase CES1A1 in the liver after absorption, and a portion of it undergoes carbonyl reduction by CYP3A4 to produce RFA, and these metabolites and their glucuronides are then excreted (Weil et al., 1988, 1990; Cornu-Chagnon et al., 1995; Miller and Spence, 1998; Fukami et al., 2010). Thus, outcomes from PK assessment could not be completely extrapolated to humans as long as interspecies differences existed in the enzymes related to FF metabolism. According to a previous report, no significant differences were reported between human and rat hepatic CES1A1 activity; furthermore, plasma PK behavior of FA in humans was in agreement with PK data in rats obtained in our study (Lovin et al., 2003; Takedani et al., 2007). Thus, FA might also exhibit high dermal exposure in humans as observed in rats. On the other hand, in humans, there appeared to be interindividual variability in PK, efficacy, and safety profiles of orally administered FF owing to the effect of food intake (Davidson et al., 2005). Yun et al. (2006) demonstrated that the oral administration of FF with a high-fat meal can cause significant increases in C_{max} and $AUC_{0-\infty}$ of FA compared with those under fasted conditions in humans; hence, the effect of food intake, especially high-fat meals, might have a major effect on the photosafety of oral FF therapy since dermal exposure of FA might be increased when FF is orally taken with high-fat meals.

To avoid undesired phototoxic events, early identification of a hazard for metabolite-mediated phototoxicity would be of great help in drug discovery. In general, to evaluate a hazard for metabolite-related toxicity without identification of metabolites, several methods have been developed based on a combination strategy of general toxicity tests and in vitro metabolism studies (Ames et al., 1973; Geissler and Faustman, 1988). As for phototoxicity, the phototoxic hazard of metabolites might be evaluated based on transitions of ROS generation from light-irradiated compounds after treatment with metabolizing enzymes, as observed in our study. However, singlet oxygen generation from some irradiated samples was negligible in the ROS assay with S9 fractions, whereas potent singlet oxygen generation from irradiated FF and FA was observed in the mROS assay. Changes in photochemical reactions in the ROS assay were attributed to assay conditions, including the concentration of chemicals and additives (Onoue et al., 2008b, 2013a, 2014b). Although further optimization of assay conditions is needed, the ROS assay employing drug-metabolizing enzymes might become a useful method for hazard identification of metabolite-mediated phototoxicity.

In conclusion, the established photosafety screening on FF with major metabolites could provide reliable photosafety information on FF. The current ICH S10 guideline for photosafety evaluation recommends conducting photochemical testing, in vitro phototoxicity assays, PK studies, and dedicated clinical studies. To avoid false prediction of drug photosafety in humans, these proposed assessments should be applied to both parent substances and their major metabolites in pharmaceutical research and development, possibly resulting in successful development of pharmaceutical products with wide safety margins.

Acknowledgments

The authors thank Philip Hawke (University of Shizuoka Scientific English Program) for critical reading of and editorial assistance with this manuscript.

Authorship Contributions

Participated in research design: Kato, Suzuki, Ohtake, Onoue.

Conducted experiments: Kato, Suzuki, Ohtake.

Contributed new reagents or analytic tools: Kato, Seto, Onoue.

Performed data analysis: Kato, Onoue.

Wrote or contributed to the writing of the manuscript: Kato, Seto, Onoue.

References

- Ames BN, Durston WE, Yamasaki E, and Lee FD (1973) Carcinogens are mutagens: a simple test system combining liver homogenates for activation and bacteria for detection. *Proc Natl Acad Sci USA* **70**:2281–2285.
- Baillie TA and Rettie AE (2011) Role of biotransformation in drug-induced toxicity: influence of intra- and inter-species differences in drug metabolism. *Drug Metab Pharmacokinet* **26**:15–29.
- Boiy A, Roelants R, van den Oord J, and de Witte PA (2008) Photosensitizing activity of hypericin and hypericin acetate after topical application on normal mouse skin. *Br J Dermatol* **158**:360–369.
- Cornu-Chagnon MC, Dupont H, and Edgar A (1995) Fenofibrate: metabolism and species differences for peroxisome proliferation in cultured hepatocytes. *Fundam Appl Toxicol* **26**:63–74.
- Davidson MH, Bays H, Rhyne J, Stein E, Rotenberg K, and Doyle R (2005) Efficacy and safety profile of fenofibrate-coated microgranules 130 mg, with and without food, in patients with hypertriglyceridemia and the metabolic syndrome: an 8-week, randomized, double-blind, placebo-controlled study. *Clin Ther* **27**:715–727.
- Drucker AM and Rosen CF (2011) Drug-induced photosensitivity: culprit drugs, management and prevention. *Drug Saf* **34**:821–837.
- Ferguson J, Addo HA, Jones S, Johnson BE, and Frain-Bell W (1985) A study of cutaneous photosensitivity induced by amiodarone. *Br J Dermatol* **113**:537–549.
- Fukami T, Takahashi S, Nakagawa N, Maruichi T, Nakajima M, and Yokoi T (2010) In vitro evaluation of inhibitory effects of antidiabetic and antihyperlipidemic drugs on human carboxylesterase activities. *Drug Metab Dispos* **38**:2173–2178.
- Geissler F and Faustman EM (1988) Developmental toxicity of aflatoxin B1 in the rodent embryo in vitro: contribution of exogenous biotransformation systems to toxicity. *Teratology* **37**:101–111.
- Henry B, Foti C, and Alsante K (2009) Can light absorption and photostability data be used to assess the photosafety risks in patients for a new drug molecule? *J Photochem Photobiol B* **96**:57–62.
- Holzthutter HG (1997) A general measure of in vitro phototoxicity derived from pairs of dose-response curves and its use for predicting the in vivo phototoxicity of chemicals. *Altern Lab Anim* **25**:445–462.
- International Conference on Harmonization of Technical Requirements for Registration of Pharmaceuticals for Human Use (ICH) (2014) ICH Safety Guideline S10 Photosafety Evaluation of Pharmaceuticals. ICH, Geneva, Switzerland. http://www.ich.org/fileadmin/Public_Web_Site/ICH_Products/Guidelines/Safety/S10/S10_Step_4.pdf
- Leenutaphong V and Manuskiatti W (1996) Fenofibrate-induced photosensitivity. *J Am Acad Dermatol* **35**:775–777.
- Ljunggren B (1977) Phenothiazine phototoxicity: toxic chlorpromazine photoproducts. *J Invest Dermatol* **69**:383–386.
- Ljunggren B and Möller H (1977) Phenothiazine phototoxicity: an experimental study on chlorpromazine and its metabolites. *J Invest Dermatol* **68**:313–317.
- Lovin I, Albu F, Tache F, David V, and Medvedovici A (2003) Solvent and salting effects on sample preparation for the determination of fenofibric acid in human plasma by HPLC-DAD. *Microchem J* **75**:179–187.
- Machet L, Vaillant L, Jan V, and Lorette G (1997) Fenofibrate-induced photosensitivity: value of photopatch testing. *J Am Acad Dermatol* **37**:808–809.
- Marković DZ, Durand T, and Patterson LK (1990) Hydrogen abstraction from lipids by triplet states of derivatized benzophenone photosensitizers. *Photochem Photobiol* **51**:389–394.
- Miller DB and Spence JD (1998) Clinical pharmacokinetics of fibric acid derivatives (fibrates). *Clin Pharmacokinet* **34**:155–162.
- Miranda MA, Boscá F, Vargas F, and Canudas N (1994) Photosensitization by fenofibrate. II. In vitro phototoxicity of the major metabolites. *Photochem Photobiol* **59**:171–174.
- Moore DE (1998) Mechanisms of photosensitization by phototoxic drugs. *Mutat Res* **422**:165–173.
- Moore DE (2002) Drug-induced cutaneous photosensitivity: incidence, mechanism, prevention and management. *Drug Saf* **25**:345–372.
- Nose T and Tsurumi K (1993) Pharmacological studies on cutaneous inflammation induced by ultraviolet irradiation (1): quantification of erythema by reflectance colorimetry and correlation with cutaneous blood flow. *Jpn J Pharmacol* **62**:245–256.
- Onoue S, Hosoi K, Wakuri S, Iwase Y, Yamamoto T, Matsuoka N, Nakamura K, Toda T, Takagi H, and Osaki N, et al. (2013a) Establishment and intra-/inter-laboratory validation of a standard protocol of reactive oxygen species assay for chemical photosafety evaluation. *J Appl Toxicol* **33**:1241–1250.
- Onoue S, Igarashi N, Yamada S, and Tsuda Y (2008a) High-throughput reactive oxygen species (ROS) assay: an enabling technology for screening the phototoxic potential of pharmaceutical substances. *J Pharm Biomed Anal* **46**:187–193.
- Onoue S, Kato M, Inoue R, Seto Y, and Yamada S (2014a) Photosafety screening of phenothiazine derivatives with combined use of photochemical and cassette-dosing pharmacokinetic data. *Toxicol Sci* **137**:469–477.
- Onoue S, Kato M, and Yamada S (2014b) Development of an albuminous reactive oxygen species assay for photosafety evaluation under experimental biomimetic conditions. *J Appl Toxicol* **34**:158–165.

- Onoue S, Seto Y, Gandy G, and Yamada S (2009) Drug-induced phototoxicity; an early in vitro identification of phototoxic potential of new drug entities in drug discovery and development. *Curr Drug Saf* **4**:123–136.
- Onoue S, Seto Y, Kato M, Aoki Y, Kojo Y, and Yamada S (2013b) Inhalable powder formulation of pirfenidone with reduced phototoxic risk for treatment of pulmonary fibrosis. *Pharm Res* **30**: 1586–1596.
- Onoue S and Tsuda Y (2006) Analytical studies on the prediction of photosensitive/phototoxic potential of pharmaceutical substances. *Pharm Res* **23**:156–164.
- Onoue S, Yamauchi Y, Kojima T, Igarashi N, and Tsuda Y (2008b) Analytical studies on photochemical behavior of phototoxic substances; effect of detergent additives on singlet oxygen generation. *Pharm Res* **25**:861–868.
- Organization for Economic Cooperation and Development (OECD) (2004) OECD Guideline for Testing of Chemicals, 432, In Vitro 3T3 NRU Phototoxicity Test, OECD, Paris. <http://ntp.niehs.nih.gov/iccvam/SuppDocs/FedDocs/OECD/OECDtg432.pdf>
- Piérard GE and Piérard-Franchimont C (1993) Dihydroxyacetone test as a substitute for the dansyl chloride test. *Dermatology* **186**:133–137.
- Roberts WC (1989) Safety of fenofibrate—US and worldwide experience. *Cardiology* **76**: 169–179.
- Seto Y, Hosoi K, Takagi H, Nakamura K, Kojima H, Yamada S, and Onoue S (2012) Exploratory and regulatory assessments on photosafety of new drug entities. *Curr Drug Saf* **7**:140–148.
- Seto Y, Inoue R, Kato M, Yamada S, and Onoue S (2013b) Photosafety assessments on pirfenidone: photochemical, photobiological, and pharmacokinetic characterization. *J Photochem Photobiol B* **120**:44–51.
- Seto Y, Inoue R, Ochi M, Gandy G, Yamada S, and Onoue S (2011) Combined use of in vitro phototoxic assessments and cassette dosing pharmacokinetic study for phototoxicity characterization of fluoroquinolones. *AAPS J* **13**:482–492.
- Seto Y, Kato M, Yamada S, and Onoue S (2013a) Development of micellar reactive oxygen species assay for photosafety evaluation of poorly water-soluble chemicals. *Toxicol In Vitro* **27**: 1838–1846.
- Seto Y, Onoue S, and Yamada S (2009) In vitro/in vivo phototoxic risk assessments of griseofulvin based on photobiochemical and pharmacokinetic behaviors. *Eur J Pharm Sci* **38**: 104–111.
- Spielmann H, Balls M, Dupuis J, Pape WJ, Pechovitch G, de Silva O, Holzhütter HG, Clothier R, Desolle P, and Gerberick F, et al. (1998) The International EU/COLIPA In Vitro Phototoxicity Validation Study: results of phase II (blind trial). Part 1: the 3T3 NRU phototoxicity test. *Toxicol In Vitro* **12**:305–327.
- Spielmann H, Gerner I, Kalweit S, Moog R, Wimsberger T, Krauser K, Kreiling R, Kreuzer H, Lüpke NP, and Miltenburger HG, et al. (1991) Interlaboratory assessment of alternatives to the Draize eye irritation test in Germany. *Toxicol In Vitro* **5**:539–542.
- Taketani M, Shii M, Ohura K, Ninomiya S, and Imai T (2007) Carboxylesterase in the liver and small intestine of experimental animals and human. *Life Sci* **81**:924–932.
- Vargas F, Canudas N, Miranda MA, and Bosca F (1993) Photodegradation and in vitro phototoxicity of fenofibrate, a photosensitizing anti-hyperlipoproteinemic drug. *Photochem Photobiol* **58**:471–476.
- Weil A, Caldwell J, and Strolin-Benedetti M (1988) The metabolism and disposition of fenofibrate in rat, guinea pig, and dog. *Drug Metab Dispos* **16**:302–309.
- Weil A, Caldwell J, and Strolin-Benedetti M (1990) The metabolism and disposition of 14C-fenofibrate in human volunteers. *Drug Metab Dispos* **18**:115–120.
- Westerhof W, van Hasselt BA, and Kammeijer A (1986) Quantification of UV-induced erythema with a portable computer controlled chromameter. *Photodermatol* **3**:310–314.
- Wójcikowski J, Boksa J, and Daniel WA (2010) Main contribution of the cytochrome P450 isoenzyme 1A2 (CYP1A2) to N-demethylation and 5-sulfoxidation of the phenothiazine neuroleptic chlorpromazine in human liver—A comparison with other phenothiazines. *Biochem Pharmacol* **80**:1252–1259.
- Yun HY, Joo Lee E, Youn Chung S, Choi SO, Kee Kim H, Kwon JT, Kang W, and Kwon KI (2006) The effects of food on the bioavailability of fenofibrate administered orally in healthy volunteers via sustained-release capsule. *Clin Pharmacokinet* **45**:425–432.

Address correspondence to: Satomi Onoue, Department of Pharmacokinetics and Pharmacodynamics, School of Pharmaceutical Sciences, University of Shizuoka, 52-1 Yada, Suruga-ku, Shizuoka 422-8526, Japan. E-mail: onoue@u-shizuoka-ken.ac.jp
